AoB PLANTS, 2019, 1–11

doi:10.1093/aobpla/plz050
Advance Access publication August 12, 2019
STUDIES

STUDIES

Stomatal anatomy coordinates leaf size with Rubisco kinetics in the Balearic *Limonium*

Miquel À. Conesa[1*], Christopher D. Muir[2], Arantzazu Molins[1,3] and Jeroni Galmés[1]

[1]Research Group on Plant Biology under Mediterranean Conditions, Departament de Biologia, INAGEA, Universitat de les Illes Balears, Carretera de Valldemossa km 7.5, E-07122 Palma, Illes Balears, Spain, [2]Department of Botany, University of Hawai'i at Mānoa, 3190 Maile Way, Honolulu, HI 96822, USA, [3]Dpto. Botánica, ICBIBE, Fac. CC. Biológicas, Universitat de València, C/Dr. Moliner 50, 46100 Burjassot, Valencia, Spain

*Corresponding authors' e-mail address: ma.conesa@uib.es

Associate Editor: Daniel Johnson

Citation: Conesa MÀ, Muir CD, Molins A, Galmés J. 2019. Stomatal anatomy coordinates leaf size with Rubisco kinetics in the Balearic *Limonium*. *AoB PLANTS* **11**: plz050; doi: 10.1093/aobpla/plz050

Abstract

Trait integration arises through both selection on functional coordination and shared developmental pathways. Different anatomical components must both work well and develop together to generate individuals with the appropriate physiology to survive and reproduce in their environment. In this study, we used a common garden experiment and Bayesian multilevel models to test whether stomatal anatomy coordinates leaf gas exchange, Rubisco kinetics and leaf size across 10 closely related species of *Limonium* from the Balearic Islands. The results indicate that the anatomical determinants of maximum stomatal conductance, stomatal density and size, were functionally coordinated with Rubisco kinetics—species whose stomatal anatomy was correlated with low stomatal conductance have evolved Rubisco enzymes better adapted to low operational chloroplastic CO_2 concentrations. Lower stomatal density was associated with greater leaf size, which can be explained by a greater proportion of pavement cells in large-leaved species. These results suggest that both selection for functional coordination (stomata and Rubisco kinetics) and shared development pathways (stomatal density and leaf area) likely shape patterns of trait integration between species.

Keywords: Drought; evolution; kinetics; leaf area; *Limonium*; Mediterranean; Rubisco; stomata; stomatal conductance.

Introduction

Plants, like all biological entities, are integrated organisms in which all parts must work well together in order to maximize fitness of the whole in a given environment. Plant leaves display many varieties of integration. For instance, the many coordinated changes in leaf anatomy and biochemistry in response to sun and shade are a canonical example (Boardman 1977; Givnish 1988). However, leaves are complex, and many hypothesized types of trait coordination are not observed consistently in nature. For example, it has long been hypothesized that thicker leaves require stomata on both surfaces to supply CO_2 (Parkhurst 1978), but this pattern is not generally strong (Mott *et al.* 1982; Muir 2015; Drake *et al.* 2019). Hence, deeper investigation into the relative role of selection on functional coordination and developmental integration are needed to understand the relative importance of each in shaping phenotypes.

As integrated organs, plant leaves must balance CO_2 supply and demand because it is costly to provision a leaf with high photosynthetic capacity (high CO_2 demand) especially if there is limited CO_2 supply. Stomatal anatomy, especially density and size, regulates gas exchange (CO_2 intake and H_2O loss) and is a significant determinant of CO_2 supply to the leaf. Theoretically, stomatal conductance (g_s, either CO_2 or H_2O) is determined by

Received: 4 May 2019; **Editorial decision:** XX XXXX XXXX; **Accepted:** 31 July 2019

stomatal density, stomatal size and the allometry between stomatal pore area and stomatal size (Franks and Beerling 2009; Sack and Buckley 2016). Fossils of plants inhabiting high to low atmospheric CO_2 concentration show a decrease in stomatal size and an increase in density, leading to higher g_s to maximize carbon gain (Franks and Beerling 2009), which appears to be reversing due to recent CO_2 rise (Woodward 1987; Lammertsma *et al.* 2011; Doheny-Adams *et al.* 2012). The positive relationship between stomatal density and conductance occurs in different environmental conditions (Woodward *et al.* 2002; Galmés *et al.* 2007; Franks *et al.* 2009).

Maximum anatomical g_s (g_{smax}) represents conductance for a given stomatal size and density in an ideal scenario assuming stomata are fully open (Franks and Farquhar 2001; Franks and Beerling 2009; Drake *et al.* 2013; Dow *et al.* 2014). Operational g_s differs from g_{smax} depending on the species and environment, but there is nevertheless a strong positive relationship between the two parameters under benign conditions (Franks *et al.* 2009; Dow *et al.* 2014). Greater stomatal density increases g_{smax}—and operational g_s—but the effect is mitigated by an inverse relationship between stomatal size and density (Hetherington and Woodward 2003; Franks and Beerling 2009; Franks *et al.* 2009). Furthermore, larger stomata have wider pores but also greater pore depth. Wider pores increase conductance compared to narrow pores for the same total pore area, but larger stomata are disadvantageous because greater pore depth lengthens the diffusion pathway of gas molecules, thereby decreasing g_{smax} (Franks and Farquhar 2007; Franks and Beerling 2009). Nevertheless, stomatal size sets the limits to g_{smax} (Franks and Beerling 2009) and pore area is adjusted by changes in pore width, since pore length is rather invariant during stomatal functioning (Lawson *et al.* 1998).

Environmental stresses such as drought induce lower stomatal conductance to conserve water, but results in lower CO_2 supply. Species adapted to photosynthesizing under chronic drought, as opposed to going dormant, are perpetually in a state of low operational CO_2 concentrations in the chloroplast (C_c) (Meinzer 1993; Chaves *et al.* 2009; Galmés *et al.* 2011), which depresses photosynthesis and exacerbates wasteful photorespiration. Many species have responded to this challenge by evolving active carbon concentrating mechanisms (C_4 and CAM) that increase the CO_2 concentration around sites of carboxylation (Sage *et al.* 2011; Edwards and Ogburn 2012). However, for C_3 species that rely on passive CO_2 diffusion, there may be other mechanisms to deal with low CO_2 concentrations. Specifically, natural selection can favour Rubisco biochemistry that increases CO_2 specificity ($S_{c/o}$), but this may come at a cost of reduced carboxylation rate (k_c^{cat}) (Galmés *et al.* 2005b, 2014b).

The resulting stomatal size and density of a fully expanded leaf do not develop in isolation, but in the context of whole leaf cell differentiation and expansion. Leaf development is initiated by cell division, followed by a phase of cell volume increase that leads to final leaf expansion (reviewed in González *et al.* 2012). Stomata and vein differentiation occur before the leaf reaches its final size (Schoch *et al.* 1980; Zwieniecki *et al.* 2004). Since leaf size is modulated by changing environment (e.g. Westoby *et al.* 2002; McDonald *et al.* 2003; Ramírez-Valiente *et al.* 2010; Yates *et al.* 2010; Carins Murphy *et al.* 2014), drought may induce correlations between leaf size with stomata and vein densities (e.g. Brodribb and Jordan 2011) or, otherwise, in a leaf size optimizing the vein to stomata ratio for a given environmental conditions (Carins Murphy *et al.* 2012). Hence, stomatal density might be 'concentrated' in smaller leaves (Gupta *et al.* 1961; Sack *et al.* 2003), whereas stomatal size appears to be much less affected by changes in leaf size and stomatal density (Sack and Frole 2006; Carins Murphy *et al.* 2012).

In parallel to adaptations to low CO_2 concentration seen from the fossil record, decreased stomatal size and increased density are also related to drought conditions, which may in turn shape correlations between drought and leaf size because of shared developmental pathways. Smaller stomata have faster and more finely tuned opening-closure regulation, allowing them to respond faster to microclimatic changes during drought, enhancing leaf water use efficiency (Aasamaa *et al.* 2001; Hetherington and Woodward 2003; Drake *et al.* 2013). Vapour pressure demand (VPD), which determines the flux of water lost through stomata, is usually high and associated with high irradiation in dry environments. Hence, small stomata that allow fast responses to changes in VPD and irradiation help prevent leaf dehydration. Stomatal density often increases with VPD (Salisbury 1928; Leuschner 2002; Lake and Woodward 2008; Hovendoven *et al.* 2012), though the opposite has also been described in several crops and cultivated plants (Bakker 1991; Torre *et al.* 2003).

We tested the hypothesis that trait integration arises because of both (i) functional coordination between stomatal and Rubisco kinetics and (ii) shared development between leaf size and stomatal density in closely related *Limonium* species from the Balearic Islands. The *Limonium* species inhabit harsh environments in the sea coast and are adapted to protracted drought (Galmés *et al.* 2005a, 2017). Under severe water-deficit (WD) conditions that would limit many plant species survivorship (Dane and Hopmans 2002), *Limonium* species show little difference in growth rate compared to a well-watered (WW) conditions, despite conserving water by decreasing stomatal conductance (Galmés *et al.* 2005a). They also vary greatly in leaf size and Rubisco kinetics. Leaf size is one of the most variable traits among *Limonium* species (Erben 1993). Further, three different Rubisco haplotypes have been described in *Limonium* (Galmés *et al.* 2014a), and most large-leaved species bear a Rubisco haplotype with the highest CO_2 specificity factor ($S_{c/o}$) and the lowest carboxylation velocity (k_c^{cat}) (Galmés *et al.* 2014a), which are characteristics expected to increase photosynthesis under low CO_2 availability conditions that occur under severe WD (Galmés *et al.* 2005b, 2014b). In fact, the different kinetics in *Limonium* have been linked to adaptations in the CO_2 delivery pathway enabling a coordination between CO_2 supply and demand, which in turn should be linked to adaptive variation in stomata (Galmés *et al.* 2017). In fact, stomatal limitations dominate over mesophyll diffusion and biochemical limitations under severe WD in *Limonium* (Galmés *et al.* 2017) and most angiosperms (Tomàs *et al.* 2013; Gago *et al.* 2014). Consequently, we hypothesize that stomatal anatomical traits constitute a key link between CO_2 supply and demand, resulting in a coordinated evolution of stomata and Rubisco in *Limonium*. Further, given its enormous variation among closely related species inhabiting the same environment, we hypothesize a key role for leaf size in explaining variation in stomatal anatomy, which could ultimately link stomatal size with Rubisco evolution in *Limonium*.

Because of their variation in stomatal anatomy, Rubisco kinetic properties and leaf size, and because the array of closely related species inhabiting the same environment, Balearic *Limonium* are ideally suited to testing the roles of selection and development in shaping trait integration. In this study, we used Bayesian multilevel models to quantify the relationships between stomatal anatomy, leaf size and Rubisco kinetics (Fig. 1) in 10 *Limonium* species, in order to deepen in understanding

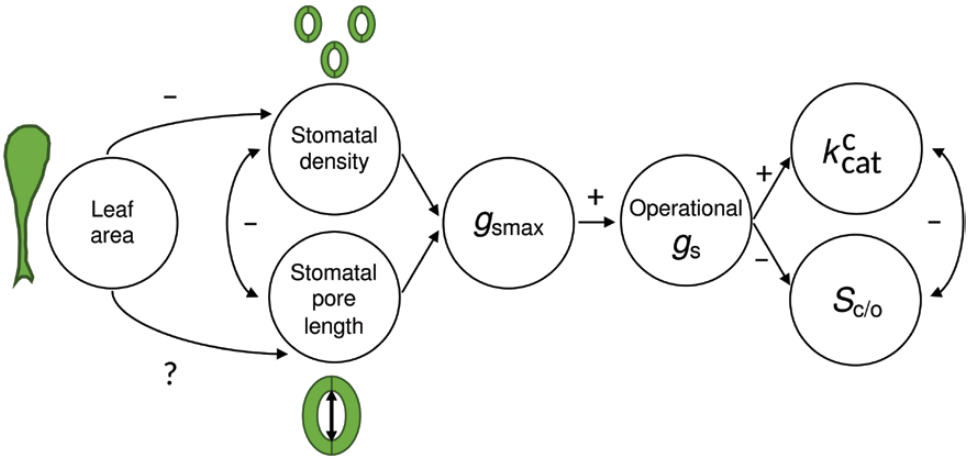

Figure 1. Conceptual overview of hypotheses and predictions. Because leaf expansion spaces out stomata, larger leaves lead to lower stomatal density but the effect on stomatal pore length is unclear. Together, stomatal density and pore length determine the anatomical maximum stomatal conductance (g_{smax}) which we predict is positively correlated with operational stomatal conductance (g_s). Lower stomatal conductance reduces the CO_2 concentration in chloroplasts, selecting for greater specificity (higher $S_{c/o}$) but reduced carboxylation activity (k_c^{cat}) due to a trade-off between specificity and rate.

the adaptive responses to severe water shortage in this fascinating group.

Materials and Methods

Species, water treatments and climatic conditions

Based on extensive sampling of *Limonium* species across the Balearic Islands, there are three distinct Rubisco large subunit gene (*rbc*L) amino acid sequences (namely haplotypes I, II and III) conferring different kinetics to the enzyme (Galmés *et al.* 2014a). In the present study, 10 species with contrasting leaf size (leaf area per leaf, LA_1) and different *rbc*L haplotype were selected (Table 1).

Field collected seeds were germinated in nurseries, and 10 plantlets per species were transplanted individually to 3 L pots and grown outdoors in spring (31 May to 28 June 2010) at the University of the Balearic Islands, irrigated at field capacity. During the following months (29 June to 13 September), five plants per species were maintained at field capacity (WW treatment). In five other plants per species, irrigation was gradually reduced to reach 30 % field capacity and maintained below this level (severe WD treatment) to the end of the experiment. Irrigation was performed every 2–3 days controlling water loss gravimetrically in order to maintain a clear difference between both water treatments. Thus, variation in % field capacity ranged between 70 % (just before irrigation) and 100 % field capacity in the WW treatment, and between 9 % (just before irrigation) and 30 % field capacity in WD treatment **[see Supporting Information—Fig. S1]**. For more details on treatment application, see Galmés *et al.* (2017).

The climatic conditions during the water treatment application period were those typical of the Mediterranean summer, with average daily temperature range (minimum–maximum) of 23.6–30.6 °C in July, 21.6–27.2 °C in August and 17.6–23.4 °C in September; and average air relative humidity range of 36–65 % in July, 45–74 % in August and 48–83 % in September. Daily sum of photosynthetically active radiation ranged 6790–15 681 μmol m^{-2} day^{-1} in July, 6500–14 615 μmol m^{-2} day^{-1} in August and 3241–11 905 μmol m^{-2} day^{-1} in September.

Table 1. *Limonium* species studied, abbreviation and their *rbc*L haplotype group.

Species	Abbreviation	*rbc*L haplotype
L. barceloi	BAR	I
L. companyonis	COM	I
L. ejulabilis	EJU	II
L. grosii	GRO	II
L. leonardi-llorensii	LEO	II
L. magallufianum	MAG	II
L. retusum	RET	II
L. antonii-llorensii	ANT	III
L. biflorum	BIF	III
L. gibertii	GIB	III

Measurements of stomatal conductance and leaf area per leaf

The stomatal conductance (g_s) and the LA_1 were measured in the last week of August, in fully expanded leaves completely developed after the water treatments were fully established.

We measured g_s in five plants per species and water treatment with a LI-6400-40 (LI-COR Inc., Lincoln, NE, USA) from 0900 to 1200 h. Gas flow was set at 250 μmol mol^{-1}, and conditions in the leaf chamber consisted of a photosynthetic photon flux density of 1500 μmol m^{-2} s^{-1}, a vapour pressure deficit of 1.2–2.5 kPa and a leaf temperature of 25 °C. The stomatal conductance was measured after steady state for at least 30 min at an ambient CO_2 concentration of 400 μmol mol^{-1}.

We measured LA_1 on five well-developed leaves per plant, and four to five plants per species and treatment. Leaves were scanned with a table scanner and leaf area was obtained from images with ImageJ (1.49v, National Institute of Health, USA).

Anatomical traits of stomata and maximum stomatal conductance

The stomatal density (*SD*), the stomatal index (*SI*) and the stomatal pore length (*SP*) were measured in four plants per species and treatment, in both the adaxial and abaxial surfaces of leaves used for leaf gas exchange and LA_1. Measurements were performed on scaled images taken with an Olympus BX60 (Tokyo, Japan) optical microscope with digital camera

incorporated. To do so, the leaf epidermis was flayed from the central-right part of the leaf blade, avoiding the midrib and main veins, and mounted on a microscope slide, keeping the sample hydrated.

For each leaf and leaf surface, an image from three different fields was taken at ×100 magnification to measure *SD* and *SI*. All epidermal cells and stomata were manually counted in each field. *SD* was expressed as number of stomata per mm^2, and *SI* was calculated as the proportion of stomata per 100 total cells. In all the fields considered for *SD*, several randomly located images were taken per field at ×500 magnification, in order to measure *SP* in at least five stomata per leaf side. To calculate total leaf *SD* and *SP*, we summed the abaxial and adaxial *SD* and averaged the abaxial and adaxial *SP* **[see Supporting Information—Methods, Fig. S2, Tables S1 and S2]**. Briefly, *SD* was similar on both surfaces, whereas *SP* was correlated but slightly smaller on the adaxial surface.

Maximum stomatal conductance to water vapour (g_{smax}) was calculated assuming fully open stomata proportions according to Franks and Beerling (2009), as modified by Sack and Buckley (2016):

$$g_{smax} = bmds^{0.5}$$

The first term is a biophysical constant equal to $b = \frac{d_w}{v}$, where the diffusivity of water vapour in air (d_w) equals 2.49 × 10^{-5} m^2 s^{-1} and the molar volume of air (v) equals 2.24 × 10^{-2} m^3 mol^{-1} at 25 °C (Monteith and Unsworth 2013). The morphological constant $m = \frac{\pi c^2}{j^{0.5}(4hj+\pi c)}$, where $c = \frac{SP}{SL} = 0.5$, $j = \frac{SW}{SL} = 0.5$ and $h = \frac{l}{SW} = 0.5$ for kidney bean-shaped guard cells. *SL* is the stomatal length, *SW* is the stomatal width and *l* is the pore depth (Sack and Buckley 2016). Stomatal density (*SD*) is equal to d in their equation. We assumed stomatal size $s = 0.5SL^2 = 0.5(2SP)^2$ (Sack and Buckley 2016). We calculated g_{smax} independently for each leaf surface. Since there was little differentiation between abaxial and adaxial stomatal traits among species **[see Supporting Information—Fig. S1, Tables S1 and S2]**, we summed values from both leaf surfaces to obtain a global g_{smax} per unit leaf surface.

Rubisco catalytic parameters

Data of Rubisco *in vitro* kinetic parameters in the 10 *Limonium* species studied were obtained from Galmés *et al.* (2014a), measured from leaves similar to the used for gas-exchange measurements.

Statistical analyses

We used three separate Bayesian statistical models to estimate (i) species-level anatomical g_{smax} and its relationship to Rubisco kinetics, (ii) the individual plant-level relationship between g_{smax} and operational g_s and (iii) the individual plant-level relationship between leaf area and stomatal traits (*SD*, *SP* and *SI*). Models 1 and 2 test predictions on functional coordination; Model 3 tests predictions on shared developmental pathways. See below for details on model fitting and significance testing.

The first model is a path analytic model (Fig. 1), in which we estimate how species and treatment impact stomatal traits (*SD* and *SP*) underlying g_{smax}, estimate a species-level average g_{smax} from the model and estimate the correlation between species-level g_{smax} and species-level Rubisco kinetic parameters k_c^{cat} and $S_{c/o}$. This procedure was required because we did not have measurements of stomata and Rubisco kinetics from the same individual plants; hence, we could only compare among species. We treated WD as a fixed effect on *SD* and *SP*, whereas species was a random effect. Besides a main effect of WD, we tested for a species-by-treatment interaction effect by comparing models with information criteria (see below for further detail). We also estimated within- and among-species correlations between *SD* and *SP*. We estimated species-level Rubisco kinetic parameters (k_c^{cat} and $S_{c/o}$) from individual replicates by treating them as a multivariate normal response with species as a random effect.

We used a Bayesian multilevel model to test for a positive relationship between anatomical g_{smax} and operational g_s (Fig. 1). We included data on individual plants, with species as a random effect. This allows us to tell whether the correlation exists among individual leaves once between-species variation is removed. Preliminary analysis found no effect of the WD treatment on the slope (results not shown), but we included a fixed effect of WD on operational g_s. We also tested for a species-by-treatment interaction effect by comparing models with information criteria (see below for further detail). To reduce skew in model residuals, we log-transformed g_s before analysis.

In the last model, we used a Bayesian multivariate multilevel model to test for the relationship between leaf area and *SD* and *SP*. We assumed the response variables (*SD* and *SP*) were multivariate Gaussian and treated LA_1 as a fixed effect and species as a random effect. Preliminary analysis found that the WD treatment had no effect on the relationship between LA_1 and stomatal anatomy (results not shown).

All three models were fit using Hamiltonian Monte Carlo in Stan version 2.18.0 (Carpenter *et al.* 2017), a language for probabilistic programming, using rstan version 2.18.2 (Stan Development Team 2018) and brms version 2.8.0 (Bürkner 2017, 2018) packages in R version 3.5.3 (R Core Team 2019). We ran all models on four chains and adjusted the number of iterations and thinning to reach convergence in all parameters (Gelman–Rubin $\hat{R} = 1$) and estimated sample size >1000. We mean-centred response variables prior to fitting and used diffuse priors on fixed effects and weakly informative priors on variance parameters, following defaults and recommendations in Stan and brms documentation. To compare models with and without species-by-treatment interactions, we used leave-one-out cross-validation information criterion (LOOIC), a generalization of Akaike Information Criterion (AIC) that makes less stringent assumptions and is more appropriate for multilevel models (Vehtari *et al.* 2017; McElreath 2018). We implemented LOOIC comparisons using the loo_compare function in brms. Where appropriate, we calculated coefficients of determination (R^2) using the bayes_R2 function in brms or custom scripts based on it. We calculated *P*-values from the posterior to test if key parameters were significantly different than zero. Finally, we report 95 % highest posterior density intervals, which are similar to confidence intervals, for key parameters. All code is available on GitHub (https://github.com/cdmuir/limonium-stomata) and will be archived on Zenodo upon publication. We performed all analysis in R. Other R packages that contributed to this work include cowplot version 0.9.4 (Wilke 2019), glue version 1.3.1 (Hester 2019), tidybayes version 1.0.4 (Kay 2019), tidyverse version 1.2.1 (Wickham 2017) and units version 0.6-2 (Pebesma *et al.* 2016).

Results

Stomatal and leaf trait data are summarized in **Supporting Information—Table S3** and Rubisco kinetic data are summarized in **Supporting Information—Table S4**.

Functional coordination between stomatal anatomy and Rubisco kinetics

We used a multilevel Bayesian path analytic model to estimate the species-level g_{smax} from measurements of stomatal density

(*SD*) and pore length (*SP*) and test whether it was associated with Rubisco kinetics. *SD* and *SP* were negatively correlated within species (r = –0.40 ± 0.10, P = 0.002), but not between species (r = 0.50 ± 0.34, P = 0.17; **see Supporting Information—Fig. S3A**). There was no main effect of the severe WD treatment on stomatal traits **[see Supporting Information—Fig. S3A–C, Table S5]**, but there was a significant treatment-by-species interaction (ΔLOOIC = 24.0 ± 10.0; **see Supporting Information—Fig. S3**). Therefore, we estimated average g_{smax} values per species in each treatment **[see Supporting Information—**Table S6**]** and correlated that with the Rubisco kinetic parameters from each species. Greater g_{smax} in both WD and WW treatments was associated with Rubisco enzymes that had greater carboxylase specific activity, k_c^{cat} (Fig. 2A), but lower specificity for CO_2, $S_{c/o}$ (Fig. 2B). The correlations were similar in both treatments, but slightly stronger in WD (Fig. 2A and B). Moreover, g_{smax} differences between WW and WD treatments were non-significant in all the species **[see Supporting Information—Fig. S4]**.

Stomatal anatomy predicts operational stomatal conductance

We estimated g_{smax} and measured g_s on 65 individual plants from all 10 *Limonium* species in both WD and WW treatments. This is fewer than the 80 total plants because we could not get both measurements from the same individual in all cases. Bayesian multilevel models revealed a positive correlation between anatomical g_{smax} and operational g_s in both treatments, but lower g_s in WD (Fig. 3; **see Supporting Information—Table S7**). Although all the species significantly reduced g_s in the WD treatment as compared to WW, there was no significant treatment-by-species interaction (ΔLOOIC = –3.2 ± 4.0; **see Supporting Information—Fig. S5**).

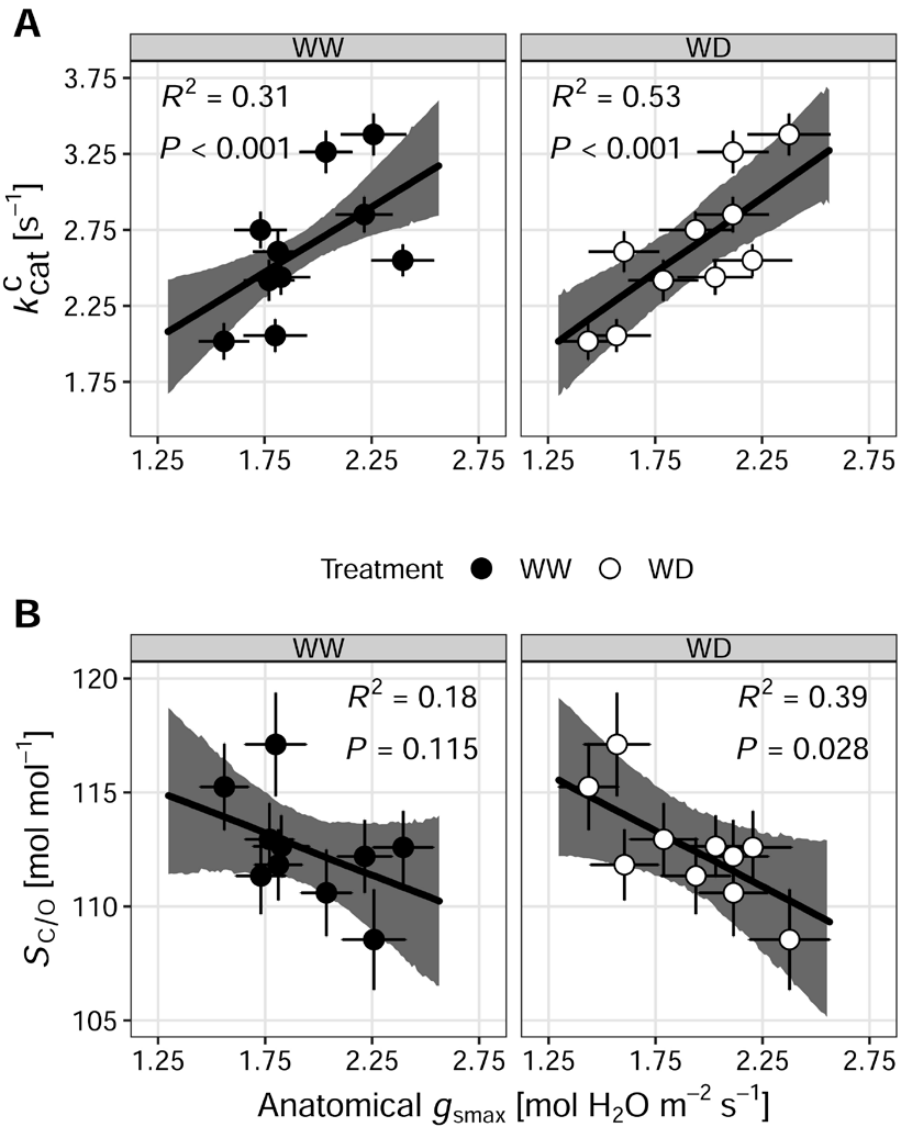

Figure 2. Greater anatomical stomatal conductance (g_{smax}) is associated with (A) greater Rubisco carboxylase activity (k_c^{cat}) but (B) reduced CO_2 specificity ($S_{c/o}$). Because anatomical responses to water treatment varied among species (see Results), we compared the species-level relationship between g_{smax} and biochemical traits in WW (left facets, black circles) and WD (right facets, white circles) treatments. The relationships are similar, but stronger under WD than WW (higher R^2 and lower P-values). Solid lines represent the median relationship between traits and grey polygons are the 95 % highest posterior density (HPD) interval from the posterior distribution. Points represent the mean value per species and bars represent the standard errors.

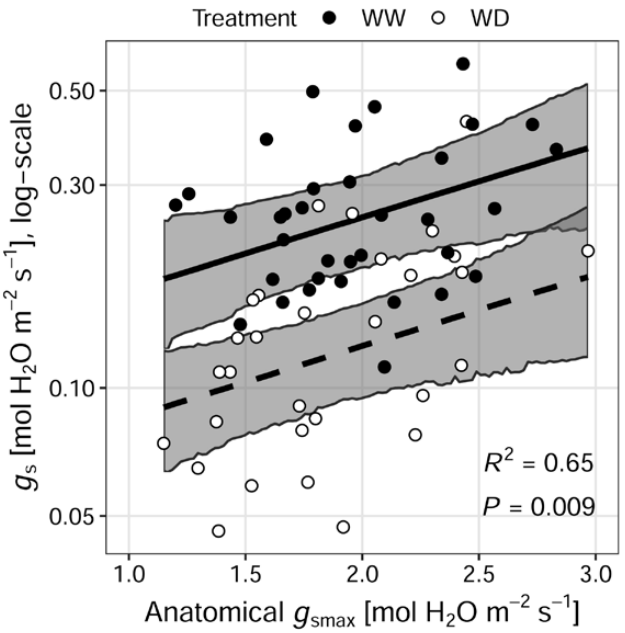

Figure 3. Anatomical maximum stomatal conductance (g_{smax}, *x*-axis) predicts operational stomatal conductance (g_s, *y*-axis, log-transformed) under both severe WD (white circles, dashed line) and WW (black circles, solid line) treatments. Anatomy determines the maximum conductance to CO_2 and water vapour (g_{smax}). As expected, species have lower stomatal conductance under WD, but the slope was not significantly different between treatments. Each point represents an individual plant from one of the 10 *Limonium* species. Grey polygons are the 95 % highest posterior density (HPD) interval from the posterior distribution.

Leaf area is associated with stomatal density, but not size

We measured leaf area and stomatal anatomical traits on 73 individual plants in all 10 *Limonium* species and under both WD and WW treatments. Again, this is fewer than the 80 total plants because we could not get both measurements from the same individual in all cases. Bayesian multivariate multilevel models showed a negative relationship between leaf area and stomatal density across both treatments (**see Supporting Information—Table S8**; Fig. 4A). In contrast, there was no significant relationship between leaf area and stomatal pore length in either treatment (Fig. 4B; **see Supporting Information—Table S8**).

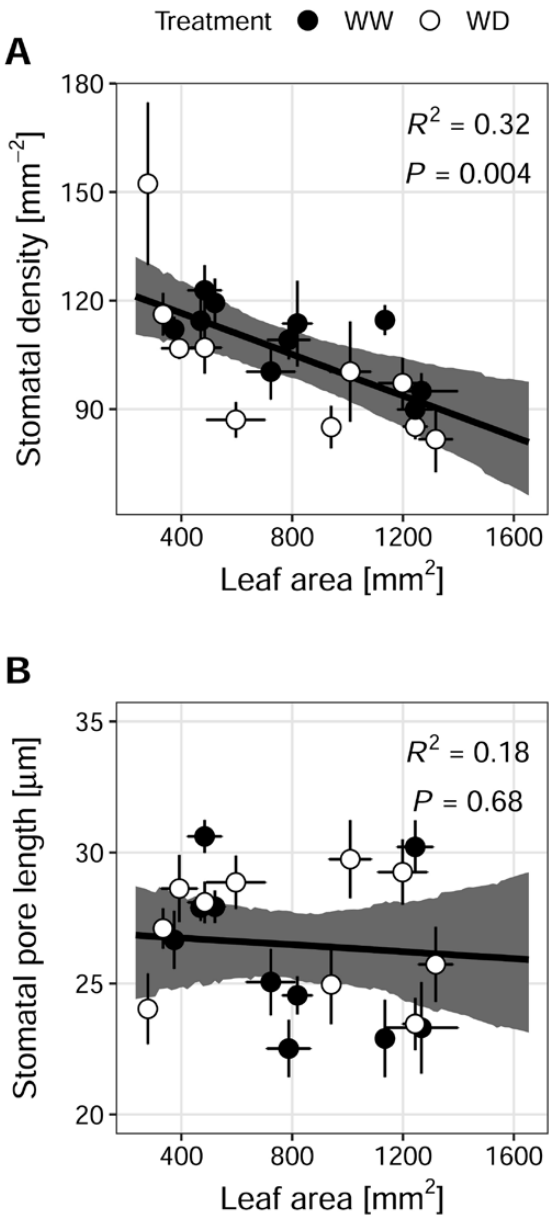

Figure 4. Larger leaves (greater leaf area) are (A) associated with greater stomatal density but (B) were not correlated with stomatal pore length in both severe WD (white points) and WW (black points) treatments. Solid lines represent the median relationship between traits and grey polygons are the 95 % highest posterior density (HPD) interval from the posterior distribution. Points represent the mean value per species and bars represent the standard errors.

Discussion

Each trait in an organism is integrated with other traits. Interspecific trait correlations can arise because of selection for functional coordination between traits and/or the developmental process affects multiple traits simultaneously. Selection will favour trait combinations that work well together and weed out trait combinations that do not. In addition, all traits arise in a developmental context, meaning they are inextricably linked with other traits through shared developmental pathways. In this study, we examined effects of both functional coordination between stomatal anatomy and Rubisco biochemistry, as well as developmental relationships between stomatal traits and leaf size. As predicted (Fig. 1), traits associated with reduced CO_2 supply were associated with Rubisco enzymes that had greater affinity for CO_2 but lower carboxylate activity (Fig. 2). Greater leaf size was associated with lower CO_2 supply because of reduced stomatal density, consistent with increased expansion of pavement cell fates driving both patterns (Fig. 4). Such findings agree with previous results in this closely related species group showing that Rubiscos operating at lower CO_2 concentration in the chloroplast (C_c) present lower carboxylation velocity and higher specificity for CO_2 (Galmés *et al.* 2017). In those species, lower C_c was a consequence of lower total conductance for CO_2. A quantitative limitation analysis of photosynthetic CO_2 assimilation showed much higher impact of stomatal than mesophyll limitations (Galmés *et al.* 2017), pointing to a key role of stomatal traits and function in the coordination between C_c and Rubisco kinetics. We conclude that both selection on functional coordination and developmental context strongly impact patterns of interspecific trait covariation.

Functional coordination between g_{smax} and Rubisco kinetics, especially under severe WD

Stomatal traits driving g_{smax} are coordinated with key biochemical traits in Rubisco kinetics across *Limonium* species (Fig. 2). Anatomical g_{smax} correlated positively with k_c^{cat} and negatively with $S_{c/o}$ in *Limonium*, consistent with a trade-off between the latter two parameters (Galmés *et al.* 2014a). Species with faster Rubisco (high k_c^{cat} and low $S_{c/o}$) have stomatal traits leading to high g_{smax}, while species with Rubisco highly specific for CO_2 have lower g_{smax}. The relationships between g_{smax} and Rubisco biochemistry were similar in both treatments (Fig. 2), reflecting that there was little plasticity in g_{smax}, with none of the species showing treatment differences in this parameter **[see Supporting Information—Fig. S4]**. Although, the g_{smax} to Rubisco biochemistry relationships were stronger under severe WD as compared to WW conditions (Fig. 2), suggesting that WD may be more relevant for understanding natural selection on Rubisco in these drought-tolerant species.

In fact, the positive correlation between g_{smax} and k_c^{cat} raises a question about why low transpiration capacity and low carboxylation velocity would be favoured by natural selection. Under severe harsh conditions, stomata closure to save water would lead to carbon starvation since low chances for CO_2 intake. Thus, species adapted to harsh conditions may have evolved towards stomatal traits reducing evaporative demand (i.e. lower density and smaller) and thus, reducing g_{smax}. However, this scenario would also lead to low CO_2 availability at the Rubisco fixation site in the chloroplast and thus, species may benefit from Rubiscos with higher efficiency in CO_2 fixation, i.e. higher $S_{c/o}$ which, given the trade-off with k_c^{cat} (Galmés *et al.* 2014a), would result in selection favouring species with lower carboxylation velocity.

Operational g_s correlates with g_{smax} in both water treatments, despite the impact of the severe WD on g_s

The similarity in the relationship of g_{smax} with kinetic traits (Fig. 2) could either indicate that WD was not severe, or that these species did not plastically adjust stomatal traits in response to severe WD. Nevertheless, *Limonium* stomatal anatomy may not be that plastic because they produce long-lived leaves that likely operate under both wet- and dry-season Mediterranean conditions. A phenotype should not be developmentally plastic if the temporal grain of the environment is finer than the organ's lifespan (Levins 1968).

Regarding the severity of WD **[see Supporting Information—Fig. S1]**, the reduction in operational g_s was evident across *Limonium* (Fig. 3), with significant differences between treatments in all the species **[see Supporting Information—Fig. S5]**, showing that WD had a strong enough impact on plant physiology. It is also worth indicating that traits other than g_s which typically denote the degree of stress, like leaf relative water content (RWC) and the quantum efficiency of PSII at predawn (F_v/F_m) and mid-morning (ϕ_{PSII}), did not parallel g_s results, and showed differences between treatments only in a few species (**see Supporting Information—Table S9**; Galmés *et al.* 2017). On the one hand, contrary to short-term stress experiments, long-term experiments like this in *Limonium* involve leaf formation under the stressful conditions and thus, leaf anatomy and structure may be modified under harsh conditions to increase chances to overcome stress limitations. This could explain the lack of differences between treatments in parameters like *RWC*, F_v/F_m and ϕ_{PSII} (**see Supporting Information—Table S9**; Galmés *et al.* 2017), despite of differences in growth (Galmés *et al.* 2014a; Conesa *et al.* 2019) and in most photosynthetic traits (Galmés *et al.* 2017) including g_s **[see Supporting Information—Fig. S5]**. The lack of differences in *RWC* can also be explained by the isohydric behaviour already described in *Limonium* (Galmés *et al.* 2007). Nevertheless, the low impact of WD on those stress-indicator parameters cannot be explained from the traits we measured, i.e. leaf size, stomatal density, stomatal size, and stomatal changes in adaxial vs. abaxial size and distribution **[see Supporting Information—Fig. S2]**, since the lack of differences between treatments across species in such traits. Further research on leaf traits involving venation density and architecture, aquaporins, osmoregulation and even hormone signalling affecting stomata, or on non-leaf traits like root characteristics, may help in fully understanding the mechanism of acclimation to severe water shortage in *Limonium*.

On the other hand, the existence of differences between treatments in g_s in all the species **[see Supporting Information—Fig. S5]**, but not in other stress-indicator parameters (**see Supporting Information—Table S9**; Galmés *et al.* 2017), denote the suitability of g_s as a stress indicator in long-term stress experiments. Over other stress-indicator parameters, including soil and plant water potentials, differences in g_s between treatments are the ultimate result after anatomical and physiological modifications facilitating acclimation to the stressful conditions, which may be variable depending on the stress and on the plant group considered. Despite the overall g_s was lower in the WD treatment, anatomical g_{smax} was positively correlated with operational g_s under both WD and WW treatments (Fig. 3). The ratio of g_s/g_{smax} in *Limonium* was on average 0.18 ± 0.01 under WW and 0.09 ± 0.01 under WD. Although the difference between operational g_s and anatomical g_{smax} depends on the species, the environment and the measuring conditions, a tight correlation between the two parameters has been described under benign conditions (Franks *et al.* 2009). Models in *Arabidopsis* estimate a g_s/g_{smax} ratio of 0.2 under common atmospheric conditions (395 ppm CO_2 and 80 % relative humidity; Dow *et al.* 2014), which is close to the 0.25 described for *Solanum pennellii* introgression lines on tomato (Fanourakis *et al.* 2015). This low ratio has been related to an optimal status of guard cells allowing fastest response to changing conditions (Franks *et al.* 2012; Dow *et al.* 2014).

Models predict that a CO_2 rise to 700 ppm by the end of the century would reduce g_s by 50 % (i.e. ca. 10 % of g_{smax}; Dow *et al.* 2014), which is close to the average for *Limonium* species under severe WD. Although it is physically possible for leaves with high anatomical g_{smax} to physiologically reduce operational g_s during drought, g_{smax} nevertheless predicts relative g_s under both benign and severe WD conditions. This could be because species with higher g_{smax} have greater hydraulic conductance, allowing them to keep stomata more open under drought (e.g. Sack *et al.* 2015), or have riskier stomatal behaviour, keeping stomata open for longer under drought to assimilate CO_2 but risking hydraulic failure (e.g. Scoffoni *et al.* 2017). Although the mechanism remains elusive from the present and past results in *Limonium*, the pattern suggests that g_{smax} is useful in predicting operational g_s under both water treatments.

Larger leaves are associated with lower stomatal density

Because epidermal cell fate is determined early in development, we predicted that larger leaves (higher LA_1) would be associated with lower *SD*, since a similar number of stomata would be spread over a larger area. There was a negative correlation between LA_1 with *SD* (Fig. 4A) but not *SP* (Fig. 4B) in both treatments. Consequently, large-leaved species 'diluted' stomatal density

by increasing the proportion of epidermal cells. Leaf size is mainly determined by cell number and not cell size at inter- and intraspecific level in plants grown in different environmental conditions (Dale 1992; Tardieu and Granier 2000). Thus, smaller leaf size is expected to result from smaller cells and to increase stomatal density due to a 'concentration' effect (Gupta 1961; Sack *et al.* 2003; Carins Murphy *et al.* 2012; Hovenden *et al.* 2012). Evidence suggests a predominant role of water availability on cell growth (Cosgrove 1986; Fricke 2002), and a limit to cell division—cell initiation—set by photosynthetic input (Pantin *et al.* 2012). In this regard, leaf size reduction has been described as a common effect of drought stress (e.g. Westoby *et al.* 2002; McDonald *et al.* 2003; Ramírez-Valiente *et al.* 2010; Yates *et al.* 2010; Carins-Murphy *et al.* 2014). Nevertheless, it is worth noting that the differences in LA_1 in *Limonium* were not related to the water treatment, but rather constitutive differences between species, which could affect adaptation to water shortage. Ultimately, this could also be related to different operational conditions of Rubisco (Fig. 1), given that the species with largest leaf size (**see Supporting Information—Table S3**; e.g. EJU, LEO, MAG, RET, but not BIF) have Rubisco haplotype II (Table 1), although it remains unknown currently. Further work with larger number of *Limonium* species could shed light on this relationship. On the other hand, LA_1 did not correlate with stomatal pore length (*SP*) across *Limonium* species and treatments (Fig. 4B), consistent with small effects of leaf size on stomatal size (Sack and Frole 2006; Carins Murphy *et al.* 2012).

Concluding remarks

Stomatal anatomy integrates Rubisco kinetics and leaf size in *Limonium* species, consistent with selection on functional coordination and shared developmental pathways. Low g_{smax} was achieved through low *SD* **[see Supporting Information—Fig. S1B]**, which we hypothesized selects for Rubisco enzymes with higher specificity for carbon but lower carboxylation rate. This finding suggests that variation in both stomatal traits and Rubisco kinetics is maintained by these trade-offs. Furthermore, low *SD* was achieved in part through larger leaf sizes (Fig. 4), implying that large-leaved *Limonium* species actually have greater water conservation (lower g_s) under severe WD. While leaf size reduction is commonly observed under harsh conditions, leaf size differences in *Limonium* are not related to acclimation to severe WD but are intrinsic species traits and thus, may better correlate to constitutive species differences like Rubisco kinetics. Moreover, the counter-intuitive leaf size response to water shortage can be explained by functional and developmental integration of anatomical, biochemical and morphological traits. Hence, organisms must be studied as integrated wholes to understand patterns of trait covariation across species.

Data

Data for this work may be found at https://github.com/cdmuir/limonium-stomata and archived at http://doi.org/10.5281/zenodo.3346025.

Supporting Information

The following additional information is available in the online version of this article—

Supporting Methods

Figure S1. Average water available in the pot as percent of field across all the *Limonium* species in the well-watered (WW; black) and severe water-deficit (WD; grey) treatments. Solid line is average for all the species, and dashed and dotted lines are maximum and minimum values among all the species, respectively. As an average for all the species, water content in 3 L pots ranged from ~70 % (just before irrigation, ~1570 g water in soil) to 100 % (just after irrigation, ~2251 g water in soil) in WW and from ~9 % (just before irrigation, ~210 g water in soil) to ~30 % (just after irrigation, ~638 g water in soil) in WD. The period shown corresponds to the days with water treatments completely established.

Figure S2. Stomatal density (Panel A) pore length (Panel B) on abaxial (*x*-axes) and adaxial (*y*-axes) leaf surfaces across *Limonium* species. Each point is the model-estimated average trait value for each of 10 species in well-watered control (WW; black circles) and severe water-deficit (WD; white circles) treatments. Bars are ±1 SE. The grey, dashed line is the 1:1 line for reference. Stomatal densities are similar on each surface (Panel A), but adaxial stomata are generally smaller than abaxial (Panel B). Regression lines are not plotted because we did not model these variables as a causal relationship, but rather as covarying within and between species. Correlation estimates and *P*-values are in Table S1.

Figure S3. Stomatal anatomy determines the maximum conductance to CO_2 and water vapour (g_{smax}). Both stomatal density (Panel B) and size (Panel C, calculated from pore length, *SP*, see Materials and Methods) strongly influence g_{smax} in both well-watered (WW; black circles) and severe water-deficit (WD; white circles) treatments. Because g_{smax} was calculated from stomatal density and size (see Materials and Methods), it is not German to include statistical tests of association (*P*-values and *r*). There was no significant correlation between density and size among species in either treatment (Panel A). Points represent the mean value per species and bars represent the standard errors.

Figure S4. Anatomical responses to severe water-deficit (WD) treatment differed among *Limonium* species (see Results). $\frac{g_{smax,WW}}{g_{smax,WD}}$ (*y*-axis) is the ratio of anatomical maximum conductances under well-watered (WW) and WD treatments. A value of 1 indicates no difference between treatments. Although model comparison indicated that species responded differently, no single species had a significant response (i.e. all 95 % highest posterior density [HPD] intervals overlap 1). Points represent the median value per species and bars represent the 95 % HPD interval. Species codes (*x*-axis) are given in Table 1.

Figure S5. Physiological responses to severe water-deficit (WD) treatment did not differ among *Limonium* species (see Results). $\frac{g_{s,WW}}{g_{s,WD}}$ (*y*-axis) is the ratio of operational stomatal conductance under well-watered (WW) and WD treatments. A value of 1 indicates no difference between treatments. Although model comparison indicated that species responded similarly, all species had a significant response (i.e. all 95 % highest posterior density [HPD] intervals do not overlap 1). Points represent the median value per species and bars represent the 95 % HPD interval. Species codes (*x*-axis) are given in Table 1.

Table S1. Abaxial and adaxial stomatal densities (*SD* [mm^{-2}]) are similar across *Limonium* species and not altered by severe water-deficit (WD) treatment. Fixed effects of the WD treatment on natural log-transformed *SD* were small and not statistically significant based on 95 % highest posterior density (HPD) intervals and *P*-values. There was no significant correlation between ab-adaxial *SD* among species, but there was within species. Other model parameters not shown.

Table S2. Stomatal pore length (*SP* [μm]) is generally larger in the abaxial than the adaxial leaf surface across *Limonium* species, but not altered by severe water-deficit (WD) treatment.

Fixed effects of the WD treatment on natural log-transformed *SP* were small and not statistically significant based on 95 % highest posterior density (HPD) intervals and *P*-values. There was no significant correlation between ab-adaxial *SP* among species, but there was within species. Other model parameters not shown.

Table S3. Stomata anatomical traits (*SD* = stomatal density, *SP* = pore length), stomatal conductance (g_s) and leaf size (leaf area per leaf, LA_1) for all the species under the well-watered (WW) and severe water-deficit (WD) treatments. Parameters shown are the sum (*SD*) or average (*SP*) of both leaf surfaces. Stomatal conductance (g_s) measured with gas-exchange analyzer under experimental conditions. Each entry gives the mean ± SE (*n*) where SE is the standard error and *n* is the sample size. Note that treatment effects (e.g. **see Supporting Information—Figs S4 and S5**) were determined for all species simultaneously from the posterior distribution of multilevel Bayesian models, not single-species SE and *n* reported in this table (see Materials and Methods for further detail). This procedure accounts for multiple comparisons, main/interaction effects and residual trait correlations which would not be captured in a species-by-species analysis. See Table 1 for species codes.

Table S4. Rubisco kinetic parameters for each species: Rubisco carboxylase specific activity (k_c^{cat}) and specificity factor ($S_{c/o}$). See Table 1 for species codes. The left columns are calculated from the raw data; the right columns beginning with 'Model' are estimated from a Bayesian multilevel model treating Species as a random effect and Rubisco kinetic parameters as correlated multivariate Gaussian responses (see Materials and Methods for further detail). Model-based parameter estimates are used in figures and statistical analyses. Each entry gives the mean ± SE (*n*) where SE is the standard error and *n* is the sample size.

Table S5. Severe water-deficit (WD) treatment had no significant effect on stomatal density (*SD*) or pore length (*SP*) in *Limonium*. Fixed effects of the WD treatment on both traits were small and not statistically significant based on 95 % highest posterior density (HPD) intervals and *P*-values. SE is the standard error. Other model parameters not shown.

Table S6. Average anatomical maximum stomatal conductance to water vapour (g_{smax} [mol H_2O m^{-2} s^{-1}]) in well-watered (WW) and severe water-deficit (WD) treatments based on Bayesian multilevel model estimates from stomatal density and size (see Materials and Methods). See Table 1 for species codes. SE is the standard error; 95 % HPD interval is the 95 % highest posterior density interval.

Table S7. Severe water-deficit (WD) treatment lowered stomatal conductance (g_s), but did not alter the effect of anatomical maximum stomatal conductance (g_{smax}) on g_s in *Limonium* based on 95 % highest posterior density (HPD) intervals and *P*-values. SE is the standard error. Other model parameters not shown.

Table S8. Greater leaf size (leaf area per leaf, LA_1) is associated lower stomatal density (*SD*) in *Limonium*, but has no effect on pore length (*SP*) based on 95 % highest posterior density (HPD) intervals and *P*-values. SE is the standard error. Other model parameters not shown.

Table S9. Indicative parameters of leaf physiological stress in the 10 species of *Limonium*, extracted from Galmés *et al.* (2017). See Table 1 for species codes. The leaf relative water content (*RWC*) and the quantum efficiency of PSII at predawn (F_v/F_m) and mid-morning (ϕ_{PSII}) were measured under well-watered (WW) and severe water-deficit (WD) treatments. Values are means ± SE (n = 3–5). Asterisks in WD indicate ANOVA significant differences between treatments within each species ($P < 0.05$).

Sources of Funding

The study was financially supported by the Spanish Ministry of Economy and Competitiveness (MINECO) projects AGL2009-07999 and AGL2013-42364-R awarded to J.G.

Contributions by the Authors

M.C. and J.G. conceived and designed the study. M.C., A.M. and J.G. performed the experiment and collected the data. C.M. did relevant Bayesian statistical analyses. M.C. and C.M. drafted the manuscript, and all authors did significant contributions to the last version and approved it.

Conflict of Interest

None declared.

Acknowledgements

We are grateful to our colleague Miquel Ribas-Carbó for Li-Cor technical assistance. We would like to thank Miquel Truyols and collaborators of the UIB Experimental Field and Greenhouses (UIBGrant 15/2015) for their support to our experiments. Trinidad Garcia is acknowledged for her technical help and organization of the radioisotope installation at the Serveis Científico-Tècnics of UIB while running these experiments.

Literature Cited

Aasamaa K, Sober A, Rahi M. 2001. Leaf anatomical characteristics associated with shoot hydraulic conductance, stomatal conductance and stomatal sensitivity to changes of leaf water status in temperate deciduous trees. *Australian Journal of Plant Physiology* **28**:765–774.

Bakker JC. 1991. Effects of humidity on stomatal density and its relation to leaf conductance. *Scientia Horticulturae* **48**:205–212.

Boardman NK. 1977. Comparative photosynthesis of sun and shade plants. *Annual Review of Plant Physiology* **28**:355–377.

Brodribb TJ, Jordan GJ. 2011. Water supply and demand remain balanced during leaf acclimation of *Nothofagus cunninghamii* trees. *The New Phytologist* **192**:437–448.

Bürkner P-C. 2017. brms: an R package for Bayesian multilevel models using Stan. *Journal of Statistical Software* **80**:1–28.

Bürkner P-C. 2018. Advanced Bayesian multilevel modeling with the R package brms. *The R Journal* **10**:395–411.

Carins Murphy MR, Jordan GJ, Brodribb TJ. 2012. Differential leaf expansion can enable hydraulic acclimation to sun and shade. *Plant, Cell & Environment* **35**:1407–1418.

Carins Murphy MR, Jordan GJ, Brodribb TJ. 2014. Acclimation to humidity modifies the link between leaf size and the density of veins and stomata. *Plant, Cell & Environment* **37**:124–131.

Carpenter B, Gelman A, Hoffman MD, Lee D, Goodrich B, Betancourt M, Brubaker M, Guo J, Li P, Riddell A. 2017. Stan: a probabilistic programming language. *Journal of Statistical Software* **76**:1–32.

Chaves MM, Flexas J, Pinheiro C. 2009. Photosynthesis under drought and salt stress: regulation mechanisms from whole plant to cell. *Annals of Botany* **103**:551–560.

Conesa MÀ, Mus M, Galmés J. 2019. Leaf size as a key determinant of contrasting growth patterns in closely related *Limonium* (Plumbaginaceae) species. *Journal of Plant Physiology* **240**:152984.

Cosgrove D. 1986. Biophysical control of plant cell growth. *Annual Review of Plant Physiology* **37**:377–405.

Dale JE. 1992. How do leaves grow? Advances in cell and molecular biology are unravelling some of the mysteries of leaf development. *Bioscience* **42**:423–432.

Dane JH, Hopmans JW. 2002. Water retention and storage. In: Dick WA, ed. *Methods of soil analysis, part 4: physical methods*. Madison, WI: Soil Science Society of America, Inc., 671–720.

Doheny-Adams T, Hunt L, Franks PJ, Beerling DJ, Gray JE. 2012. Genetic manipulation of stomatal density influences stomatal size, plant growth and tolerance to restricted water supply across a growth carbon dioxide gradient. *Philosophical Transactions of the Royal Society B* **367**:547–555.

Dow GJ, Bergmann DC, Berry JA. 2014. An integrated model of stomatal development and leaf physiology. *The New Phytologist* **201**:1218–1226.

Drake PL, de Boer HJ, Schymanski SJ, Veneklaas EJ. 2019. Two sides to every leaf: water and CO_2 transport in hypostomatous and amphistomatous leaves. *The New Phytologist*. doi:10.1111/nph.15652.

Drake PL, Froend RH, Franks PJ. 2013. Smaller, faster stomata: scaling of stomatal size, rate of response, and stomatal conductance. *Journal of Experimental Botany* **64**:495–505.

Erben M. 1993. *Limonium*. In: Castroviejo S, Aedo C, Cirujano S, Lainz M, Monserrat P, Morales R, Muñoz F, Navarro C, Paiva J, Soriano C, eds. *Flora Iberica*, vol. 3. Madrid: Real Jardín Botánico-CSIC, 2–143.

Edwards EJ, Ogburn RM. 2012. Angiosperm responses to a low-CO_2 world: CAM and C_4 photosynthesis as parallel evolutionary trajectories. *International Journal of Plant Sciences* **173**:724–733.

Fanourakis D, Giday H, Milla R, Pieruschka R, Kjaer KH, Bolger M, Vasilevski A, Nunes-Nesi A, Fiorani F, Ottosen CO. 2015. Pore size regulates operating stomatal conductance, while stomatal densities drive the partitioning of conductance between leaf sides. *Annals of Botany* **115**:555–565.

Franks PJ, Beerling DJ. 2009. Maximum leaf conductance driven by CO_2 effects on stomatal size and density over geologic time. *Proceedings of the National Academy of Sciences of the United States of America* **106**:10343–10347.

Franks PJ, Drake PL, Beerling DJ. 2009. Plasticity in maximum stomatal conductance constrained by negative correlation between stomatal size and density: an analysis using *Eucalyptus globulus*. *Plant, Cell & Environment* **32**:1737–1748.

Franks PJ, Farquhar GD. 2001. The effect of exogenous abscisic acid on stomatal development, stomatal mechanics, and leaf gas exchange in *Tradescantia virginiana*. *Plant Physiology* **125**:935–942.

Franks PJ, Farquhar GD. 2007. The mechanical diversity of stomata and its significance in gas-exchange control. *Plant Physiology* **143**:78–87.

Franks PJ, Leitch IJ, Ruszala EM, Hetherington AM, Beerling DJ. 2012. Physiological framework for adaptation of stomata to CO_2 from glacial to future concentrations. *Philosophical Transactions of the Royal Society B* **367**:537–546.

Fricke W. 2002. Biophysical limitation of cell elongation in cereal leaves. *Annals of Botany* **90**:157–167.

Gago J, Douthe C, Florez-Sarasa I, Escalona JM, Galmes J, Fernie AR, Flexas J, Medrano H. 2014. Opportunities for improving leaf water use efficiency under climate change conditions. *Plant Science* **226**:108–119.

Galmés J, Andralojc PJ, Kapralov MV, Flexas J, Keys AJ, Molins A, Parry MA, Conesa MÀ. 2014a. Environmentally driven evolution of Rubisco and improved photosynthesis and growth within the C_3 genus *Limonium* (Plumbaginaceae). *The New Phytologist* **203**:989–999.

Galmés J, Cifre J, Medrano H, Flexas J. 2005a. Modulation of relative growth rate and its components by water stress in Mediterranean species with different growth forms. *Oecologia* **145**:21–31.

Galmés J, Flexas J, Keys AJ, Cifre J, Mitchell RAC, Madgwick PJ, Haslam RP, Medrano H, Parry MAJ. 2005b. Rubisco specificity factor tends to be larger in plant species from drier habitats in species with persistent leaves. *Plant, Cell and Environment* **28**:571–579.

Galmés J, Flexas J, Savé R, Medrano H. 2007. Water relations and stomatal characteristics of Mediterranean plants with different growth forms and leaf habits: responses to water stress and recovery. *Plant and Soil* **290**:139–155.

Galmés J, Kapralov MV, Andralojc PJ, Conesa MÀ, Keys AJ, Parry MA, Flexas J. 2014b. Expanding knowledge of the Rubisco kinetics variability in plant species: environmental and evolutionary trends. *Plant, Cell & Environment* **37**:1989–2001.

Galmés J, Molins A, Flexas J, Conesa MÀ. 2017. Coordination between leaf CO2 diffusion and Rubisco properties allows maximizing photosynthetic efficiency in *Limonium* species. *Plant, Cell & Environment* **40**:2081–2094.

Galmés J, Ribas-Carbó M, Medrano H, Flexas J. 2011. Rubisco activity in Mediterranean species is regulated by the chloroplastic CO_2 concentration under water stress. *Journal of Experimental Botany* **62**:653–665.

Givnish TJ. 1988. Adaptation to sun and shade: a whole-plant perspective. *Australian Journal of Plant Physiology* **15**:63–92.

Gonzalez N, Vanhaeren H, Inzé D. 2012. Leaf size control: complex coordination of cell division and expansion. *Trends in Plant Science* **17**:332–340.

Gupta B. 1961. Correlation of tissues in leaves. 1. Absolute vein-islet numbers and absolute veinlet termination numbers. *Annals of Botany* **25**:65–70.

Hester J. 2019. *glue: interpreted string literals*. *R package version* 1.3.1. https://CRAN.R-project.org/package=glue (12 March 2019).

Hetherington AM, Woodward FI. 2003. The role of stomata in sensing and driving environmental change. *Nature* **424**:901–908.

Hovenden MJ, Vander Schoor JK, Osanai Y. 2012. Relative humidity has dramatic impacts on leaf morphology but little effect on stomatal index or density in *Nothofagus cunninghamii* (Nothofagaceae). *Australian Journal of Botany* **60**:700–706.

Kay M. 2019. *tidybayes: tidy data and geoms for Bayesian models*. *R package version* 1.0.4. doi:10.5281/zenodo.1308151.

Lake JA, Woodward FI. 2008. Response of stomatal numbers to CO_2 and humidity: control by transpiration rate and abscisic acid. *The New Phytologist* **179**:397–404.

Lammertsma EI, de Boer HJ, Dekker SC, Dilcher DL, Lotter AF, Wagner-Cremer F. 2011. Global CO_2 rise leads to reduced maximum stomatal conductance in Florida vegetation. *Proceedings of the National Academy of Sciences of the United States of America* **108**:4035–4040.

Lawson T, James W, Weyers J. 1998. A surrogate measure of stomatal aperture. *Journal of Experimental Botany* **49**:1397–1403.

Leuschner C. 2002. Air humidity as an ecological factor for woodland herbs: leaf water status, nutrient uptake, leaf anatomy, and productivity of eight species grown at low or high VPD levels. *Flora* **197**:262–274.

Levins R. 1968. *Evolution in changing environments: some theoretical explorations*. Princeton, NJ: Princeton University Press.

McDonald PG, Fonseca CR, Overton MC, Westoby M. 2003. Leaf-size divergence along rainfall and soil-nutrient gradients: is the method of size reduction common among clades? *Functional Ecology* **17**:50–57.

McElreath R. 2016. *Statistical rethinking: a Bayesian course with examples in R and Stan*. Boca Raton, FL: Chapman and Hall.

Meinzer FC. 1993. Stomatal control of transpiration. *TREE* **8**:267–305.

Monteith JL, Unsworth MH. 2013. *Principles of environmental physics*, 4th edn. Oxford: Academic Press.

Mott KA, Gibson AC, O'Leary JW. 1982. The adaptive significance of amphistomatic leaves. *Plant, Cell and Environment* **5**:455–460.

Muir CD. 2015. Making pore choices: repeated regime shifts in stomatal ratio. *Proceedings of the Royal Society B* **282**:20151498.

Pantin F, Simonneau T, Muller B. 2012. Coming of leaf age: control of growth by hydraulics and metabolics during leaf ontogeny. *The New Phytologist* **196**:349–366.

Parkhurst DF. 1978. The adaptive significance of stomatal occurrence on one or both surfaces of leaves. *The Journal of Ecology* **66**:367–383.

Pebesma E, Mailund T, Hiebert J. 2016. Measurement units in R. *The R Journal* **8**:486–494.

Ramírez-Valiente JA, Sánchez-Gómez D, Aranda I, Valladares F. 2010. Phenotypic plasticity and local adaptation in leaf ecophysiological traits of 13 contrasting cork oak populations under different water availabilities. *Tree Physiology* **30**:618–627.

R Core Team. 2019. *R: a language and environment for statistical computing*. Vienna, Austria: R Foundation for Statistical Computing.

Sack L, Buckley TN. 2016. The developmental basis of stomatal density and flux. *Plant Physiology* **171**:2358–2363.

Sack L, Cowan PD, Jaikumar N, Holbrook NM. 2003. The 'hydrology' of leaves: co-ordination of structure and function in temperate woody species. *Plant, Cell and Environment* **26**:1343–1356.

Sack L, Frole K. 2006. Leaf structural diversity is related to hydraulic capacity in tropical rain forest trees. *Ecology* **87**:483–491.

Sack L, Scoffoni C, Johnson DM, Buckley TN, Brodribb TJ. 2015. The anatomical determinants of leaf hydraulic function. In: Hacke U, ed. *Functional and ecological xylem anatomy*. Cham, Switzerland: Springer International Publishing, 255–271.

Sage RF, Christin PA, Edwards EJ. 2011. The C_4 plant lineages of planet Earth. *Journal of Experimental Botany* **62**:3155–3169.

Salisbury EJ. 1928. On the causes and ecological significance of stomatal frequency, with special reference to the woodland flora. *Philosophical Transactions of the Royal Society B* **216**:1–65.

Schoch PG, Zinsou C, Sibi M. 1980. Dependence of stomatal index on environmental factors during stomata differentiation in leaves of *Vigna signensis* L. *Journal of Experimental Botany* **31**:1211–1216.

Scoffoni C, Albuquerque C, Brodersen CR, Townes SV, John GP, Bartlett MK, Buckley TN, McElrone AJ, Sack L. 2017. Outside-xylem vulnerability, not xylem embolism, controls leaf hydraulic decline during dehydration. *Plant Physiology* **173**:1197–1210.

Stan Development Team. 2018. *RStan: the R interface to Stan. R package version* 2.18.2. http://mc-stan.org/ (1 November 2018).

Tardieu F, Granier C. 2000. Quantitative analysis of cell division in leaves: methods, developmental patterns and effects of environmental conditions. *Plant Molecular Biology* **43**:555–567.

Tomás M, Flexas J, Copolovici L, Galmés J, Hallik L, Medrano H, Ribas-Carbó M, Tosens T, Vislap V, Niinemets Ü. 2013. Importance of leaf anatomy in determining mesophyll diffusion conductance to CO_2 across species: quantitative limitations and scaling up by models. *Journal of Experimental Botany* **64**:2269–2281.

Torre S, Fjeld T, Gislerød HR, Moe R. 2003. Leaf anatomy and stomatal morphology of greenhouse roses grown at moderate or high air humidity. *Journal of the American Society for Horticultural Science* **128**:598–602.

Vehtari A, Gelman A, Gabry J. 2017. Practical Bayesian model evaluation using leave-one-out cross-validation and WAIC. *Statistics and Computing* **27**:1413–1432.

Westoby M, Falster DS, Moles AT, Vesk PA, Wright IJ. 2002. Plant ecological strategies: some leading dimensions of variation 652 between species. *Annual Review of Ecology and Systematics* **33**:125–159.

Wickham H. 2017. *tidyverse: easily install and load the 'tidyverse'. R package version* 1.2.1. https://CRAN.R-project.org/package=tidyverse (14 November 2017).

Wilke CO. 2019. *cowplot: streamlined plot theme and plot annotations for 'ggplot2'. R package version* 0.9.4. https://CRAN.R-project.org/package=cowplot (7 January 2019).

Woodward FI. 1987. Stomatal numbers are sensitive to increases in CO_2 from pre-industrial levels. *Nature* **327**:617–618.

Woodward FI, Lake JA, Quick WP. 2002. Stomatal development and CO_2: ecological consequences. *The New Phytologist* **153**:477–484.

Yates MJ, Verboom GA, Rebelo AG, Cramer MD. 2010. Ecophysiological significance of leaf size variation in Proteaceae from the Cape Floristic Region. *Functional Ecology* **24**:485–492.

Zwieniecki MA, Boyce CK, Holbrook NM. 2004. Functional design space of single-veined leaves: role of tissue hydraulic properties in constraining leaf size and shape. *Annals of Botany* **94**:507–513.